

Theory for the early stages of phase separation: The long-range-force limit

Martin Grant, M. San Miguel,* J. Viñals, and J. D. Gunton
Physics Department, Temple University, Philadelphia, Pennsylvania 19122
 (Received 17 September 1984)

A systematic perturbation theory for the early stages of spinodal decomposition is developed for systems with long-range forces. The small parameter in our theory is proportional to the inverse of the range of the force. The Cahn-Hilliard-Cook theory for the structure factor results as the leading term in the expansion. The first-order perturbative correction to that result, as expected, acts to substantially slow down the evolution predicted by the earlier theory of Cahn *et al.* Coupling of wave-number modes, not given in previous theories, is a natural consequence of our theory. We also find that one cannot consistently define a spinodal curve for systems with a finite range of force: The effective "critical wave number" which determines this curve becomes time dependent. The theoretical results we obtain could be tested experimentally on systems with long-range forces, such as polymer-polymer blends or some binary alloys.

I. INTRODUCTION

A disordered system quenched from a high initial temperature to a final one, below its critical point, evolves to its ordered equilibrium state in different stages.¹⁻⁴ In spinodal decomposition the system is initially unstable with respect to long-wavelength fluctuations. Hence, an interconnected structure forms which coarsens during the early stages.⁵⁻¹⁰ For later times, well-defined domains form which evolve via interfacial dynamics.¹¹ In this paper we study the early stages of spinodal decomposition.

The well-known Cahn-Hilliard-Cook theory of spinodal decomposition describes some aspects of those early stages.⁵⁻⁷ It consists of a linear stability analysis of the initially disordered state, and correctly predicts the long-wavelength instability. A sharp distinction between unstable and metastable states, given by the classical spinodal curve, is predicted by this analysis. Historically, the theory of Cahn *et al.* has provided a useful guide for experimentalists. The theory, however, cannot account for intrinsically nonlinear effects occurring in the later stages, such as coarsening.

Many theories have attempted to incorporate nonlinear effects into a theory of spinodal decomposition. Langer and co-workers⁸⁻¹⁰ have presented the most successful theories to date. They undertake physical (but uncontrolled) approximations which account for those nonlinearities. In particular, Langer, Bar-on, and Miller's¹⁰ theory quantitatively accounts for nonlinear effects which result in coarsening during the initial break up of the interconnected structure. Nonetheless, these and related theories cannot be systematically improved because they involve no small parameter, since, for example, they consider systems with short-ranged forces.

Thus an important issue is to determine the precise regime of validity of the linear Cahn-Hilliard-Cook theory. Patashinskii and Pokrovskii,¹² and more recently, Binder,¹³ have identified this through a modified Ginzburg criteria. It is found that the theory of Cahn *et al.* is most valid for systems with a long range of force.

Explicitly, the time regime over which that theory is valid is proportional to the logarithm of the range of the interaction. Many systems with effectively long-range forces exist in nature, for example, FeCr.^{14,15} Snyder, Meakin, and Reich,¹⁶ and Russell and co-workers,¹⁷ have recently studied phase separation in polymer-polymer blends, and have found reasonable agreement with Cahn-Hilliard-Cook theory over early times.¹⁸⁻²⁰ Similar early-time agreement has been found by Heermann²¹ in a numerical simulation of a long-range-force kinetic Ising model.

Our concern in this paper is with spinodal decomposition in systems with long-range forces. For such systems a small parameter exists: the inverse of the range of the force. This allows us to construct a systematic perturbation theory. A distinctive feature of our theory, compared to previous work, is that it incorporates the coupling of different Fourier modes of the order parameter. This could be important for the description of the interconnected structure unique to the early stages of spinodal decomposition. The first nonvanishing term in this expansion yields the Cahn-Hilliard-Cook result for the structure factor. The next order contribution produces a qualitative change to the result of linear theory, due to nonlinear effects. While the direct perturbative treatment is restricted to the early stages of spinodal decomposition, we expect that our results should be experimentally observable over an important time domain for systems with effectively long-range forces. For systems with an intermediate range of the interaction, our analysis applies to a more restricted time domain.

The results of our calculation, for a symmetric quench of a binary-alloy model, indicate, as expected, that the correction terms to the Cahn-Hilliard-Cook theory considerably slow down the growth of the unstable modes. Coarsening, which is absent from the linear theory, follows from our calculation. Another interesting effect we obtain is the "crossing of the tails" of the structure factor for different times (Sec. V), which has been observed in numerical and experimental studies of phase separa-

tion.²²⁻²⁵ Finally, we find that, for systems with a finite range of interaction, there is no way to consistently define a sharp spinodal curve.³ We find that the effective "critical wave number," which gives the position of the spinodal curve, becomes time dependent. Thus the spinodal curve only appears to be a useful concept for dynamics in the limit of an infinite range of interaction. This result is in agreement with experimental and theoretical studies which find a gradual transition between unstable and metastable states.²¹⁻³¹

The outline of the remainder of this paper is as follows. In Sec. II we introduce the model used in our calculation and briefly review earlier theories of spinodal decomposition. In Sec. III we identify the small parameter and outline our perturbation expansion. The calculation to first order is given in Sec. IV. Section V contains a discussion of our results.

II. MOTIVATION

In this section we briefly survey some previous well-known work on the early to intermediate stages of phase separation. This will serve to fix notation, and to provide a background for the present work. Our starting point consists of a simplified dynamical model of a binary alloy which is called model *B* in critical dynamics,³² and is commonly used in the study of spinodal decomposition.⁵⁻¹⁰ The time evolution of the scalar-conserved order parameter $\phi(\mathbf{r}, t)$ is given by

$$\frac{\partial \phi}{\partial t}(\mathbf{r}, t) = M \nabla^2 \frac{\delta F}{\delta \phi(\mathbf{r}, t)} + \xi(\mathbf{r}, t), \quad (2.1)$$

where M is the (constant) mobility and ϕ is related to the concentration c through $\phi = c - c_{cr}$, where c_{cr} is the critical concentration. The "coarse-grained" free-energy functional is assumed to be given by

$$F[\phi] = \int d^d r \left[\frac{K}{2} (\nabla \phi)^2 + f(\phi) \right], \quad (2.2)$$

in d dimensions. Herein K gives the range over which spatial inhomogeneities can persist, with $K \propto R^2$, where R is the range of the force. In the two-phase region, below the critical temperature T_c , the bulk free-energy density is given by

$$f(\phi) = -\frac{r}{2} \phi^2 + \frac{u}{4} \phi^4 + \dots, \quad (2.3)$$

where r and u are positive constants (r should not be confused with the spatial position \mathbf{r}). The Gaussian thermal noise, $\xi(\mathbf{r}, t)$, satisfies the usual fluctuation-dissipation relation,

$$\langle \xi(\mathbf{r}, t) \xi(\mathbf{r}', t') \rangle = -2k_B T M \nabla^2 \delta(\mathbf{r} - \mathbf{r}') \delta(t - t'), \quad (2.4)$$

where k_B is Boltzmann's constant and T is the temperature. As discussed in the Introduction, we are primarily concerned with systems which have relatively long-range forces. One such example is essentially provided by polymer-polymer blends, for which the Flory-Huggins free-energy density is¹³

$$f(c) = \frac{c}{N_A} \ln c + \frac{1-c}{N_B} \ln(1-c) + v c(1-c), \quad (2.5)$$

where c is now the volume fraction of one of the two species. The chain lengths are given by N_A and N_B , respectively, while v is the effective interaction parameter. If one expands Eq. (2.5) about the critical point, Eq. (2.3) is recovered, with specific values for r and u .³³ We will consider an instantaneous quench from a one-phase, disordered state to an unstable state within the two-phase coexistence region. Our work deals only with the early stages of phase separation following the quench.

The first theory of spinodal decomposition is due to Cahn and Hilliard,^{5,6} later modified to account for thermal fluctuations by Cook.⁷ Consider a symmetric quench, where $\phi=0$ initially. In the Cahn-Hilliard-Cook theory one linearizes around this value and obtains from Eq. (2.1),

$$\frac{\partial \phi}{\partial t} = -MK \nabla^2 (\nabla^2 + q_c^2) \phi + \xi, \quad (2.6)$$

where

$$q_c^2 = \frac{r}{K} \quad (2.7)$$

is called the critical wave number. If we introduce the Fourier transformation

$$\phi(\mathbf{q}, t) = \int d^d r e^{i\mathbf{q}\cdot\mathbf{r}} \phi(\mathbf{r}, t), \quad (2.8)$$

then we obtain the two-point correlation function

$$\langle \phi(\mathbf{q}, t) \phi(\mathbf{q}', t) \rangle = (2\pi)^d \delta(\mathbf{q} + \mathbf{q}') \langle |\phi|^2 \rangle(\mathbf{q}, t), \quad (2.9)$$

where the structure factor is given by

$$\begin{aligned} \langle |\phi^2| \rangle(\mathbf{q}, t) &= \langle |\phi^2| \rangle(\mathbf{q}, 0) \exp[2MKq^2(q_c^2 - q^2)t] \\ &\quad - \frac{k_B T}{K(q_c^2 - q^2)} \{1 - \exp[2MKq^2(q_c^2 - q^2)t]\}. \end{aligned} \quad (2.10)$$

As discussed below, $\langle |\phi|^2 \rangle(\mathbf{q}, t=0)$ is well approximated by the Ornstein-Zernike function in the high-temperature phase. Note that the system is unstable for wave numbers $q < q_c$. Thus the linear stability analysis allows one to identify the existence of the instability, and predicts exponential growth for long wavelengths. This instability results in an interconnected structure which is characteristic of spinodal decomposition. It should be noted that if we linearize around an off-symmetric initial condition (where $\phi = \phi_0$ at $t=0$) then the critical wave number becomes

$$q_c^2 = \frac{r}{K} - 3\phi_0^2. \quad (2.11)$$

Thus q_c can vanish for an off-symmetric quench (where $\partial^2 f / \partial \phi^2 = 0$) in the linear theory, and the long-wavelength instability disappears. This sharp limit of instability denotes the classical spinodal line which separates unstable states from metastable states.

The spinodal curve has been the subject of a great deal of study.^{3,24-31} It is usually presented as part of the equilibrium phase diagram,⁴ although it is associated with far-from-equilibrium dynamical processes. In dynamical studies, experimentalists search for this quantity by plot-

ting $(1/q^2 t) \ln \langle |\phi|^2 \rangle$ versus q^2 . In the absence of the Cook term [the last quantity on the right-hand side of Eq. (2.10)] Cahn-Hilliard theory predicts that this plot will give a straight line. The intercepts of this line determine the position of the spinodal.

As is well known, the Cahn-Hilliard-Cook theory has some serious deficiencies. These are all related to the fact that it does not describe the correct two-phase equilibrium solution. In particular, the one-body distribution function (which determines the spatially averaged order parameter) remains Gaussian centered on $\phi = \phi_0$, with a variance which grows exponentially in time.³⁴ We will discuss the domain of validity in time of the theory of Cahn *et al.* in the following section.

To go beyond this theory obviously requires consideration of nonlinear effects. We now turn to the equation of motion for the structure factor. From Eq. (2.1), one obtains

$$\begin{aligned} \frac{\partial}{\partial t} \langle \phi(\mathbf{r}, t) \phi(\mathbf{r}', t) \rangle &= -2M \nabla^2 (r + K \nabla^2) \langle \phi(\mathbf{r}, t) \phi(\mathbf{r}', t) \rangle \\ &\quad + 2Mu \nabla^2 \langle \phi^3(\mathbf{r}, t) \phi(\mathbf{r}', t) \rangle \\ &\quad - 2Mk_B T \nabla^2 \delta(\mathbf{r} - \mathbf{r}'), \end{aligned} \quad (2.12)$$

which is formally exact. Clearly this equation of motion is coupled to that for $\langle \phi^3(\mathbf{r}, t) \phi(\mathbf{r}', t) \rangle$ so that Eq. (2.12) is the first of a hierarchy of equations of motion. There are two types of coupling present in this hierarchy, one due to the nonlinearities and one due to the gradients.

Several attempts have been made to obtain approximate solutions of the hierarchy of equations corresponding to Eq. (2.12).⁸⁻¹⁰ Most of these have dealt with the issue of the nonlinear coupling and its role in the coarsening mechanism. One approach, due to Langer,⁹ is to factorize the nonlinear terms by a Gaussian approximation so that

$$\nabla^2 \langle \phi^3(\mathbf{r}, t) \phi(\mathbf{r}', t) \rangle \approx \nabla^2 [3 \langle \phi^2(\mathbf{r}, t) \rangle \langle \phi(\mathbf{r}, t) \phi(\mathbf{r}', t) \rangle], \quad (2.13)$$

for example. The result of this is an equation of motion for the structure factor with the same spatial dependence as the earlier Cahn-Hilliard-Cook theory but with q_c in Eq. (2.12) replaced by a time-dependent quantity $A(t)$. Thus, roughly speaking, wave numbers $q < A(t)$ are again unstable, but since it turns out that $A(t)$ decreases with time, the equilibration process is more physical than in the linear theory. The most important result of this approximation is a qualitative explanation of coarsening. It should be noted that the distribution function, by assumption, remains a time-dependent Gaussian.

A subsequent approximation scheme was given by Langer, Bar-on, and Miller.¹⁰ By assuming a form for the two-body distribution function, they were able to close the hierarchy relating the many-body distributions. Their theory yields a bimodal distribution (rather than a single Gaussian), and is the most successful "early-time" theory yet available. Discussions of its limitations have been given elsewhere.³⁵

Neither of these nonlinear theories is systematic, since there is no smallness parameter. As well, neither theory

deals with the coupling arising from gradients in the equations of motion: both theories lead to an equation of motion for the structure factor of the Cahn-Hilliard-Cook form, with a time-dependent wave number $A(t)$ replacing q_c , but with no coupling between different Fourier components of the order parameter. In the next section we identify a small parameter for systems with a long range of interaction, and show how the coupling of wave-number modes arises in our theory.

III. PERTURBATION EXPANSION IN THE RANGE OF THE FORCE

We now present a theory of the early stages of spinodal decomposition. This involves a systematic solution of the hierarchy of equations of motion, of which Eq. (2.12) is the first, by an expansion in the inverse of the range of the force. The perturbative treatment enables us to make several connections to previous work: the leading term gives the Cahn-Hilliard-Cook theory; the next order term in the expansion yields a time-dependent one-point Gaussian distribution function. This Gaussian form is the result of the theory, rather than an ansatz as in Langer's factorization approximation [Eq. (2.13)] (Ref. 9) and, indeed, the Gaussian distribution we obtain differs from that of Langer. The expansion itself is closely related to Kawasaki's³⁶ formal expansion in the nonlinear coupling parameter u in Eq. (2.3).

A. Scaling, expansion parameter, and initial conditions

It is convenient to scale the equations in the following manner:

$$\mathbf{x} = \left[\frac{r}{K} \right]^{1/2} \mathbf{r}, \quad (3.1)$$

$$\tau = 2 \frac{Mr^2}{K} t, \quad (3.2)$$

and

$$\psi = \left[\frac{u}{r} \right]^{1/2} (\phi - \phi_0). \quad (3.3)$$

The resulting Langevin equation for ψ is

$$\frac{\partial \psi}{\partial \tau} = \frac{1}{2} \nabla^2 (-\nabla^2 \psi - q_c^2 \psi + 3\psi_0 \psi^2 + \psi^3) + \sqrt{\epsilon} \mu, \quad (3.4)$$

where the intensity of the noise is given by

$$\epsilon \equiv \frac{k_B T u}{r^2} \left[\frac{r}{K} \right]^{d/2}, \quad (3.5)$$

and we have introduced

$$q_c^2 \equiv 1 - 3\psi_0^2 \quad (3.6)$$

and

$$\psi_0 = \left[\frac{u}{r} \right]^{1/2} \phi_0. \quad (3.7)$$

Note that $\psi_0 = 0$ corresponds to a symmetric quench while $\psi_0 = \pm 1/\sqrt{3}$ yields the classical spinodal curve. The

Gaussian noise is now determined by

$$\langle \mu(\mathbf{x}, \tau) \mu(\mathbf{x}', \tau') \rangle = -\nabla^2 \delta(\mathbf{x} - \mathbf{x}') \delta(\tau - \tau'). \quad (3.8)$$

The theory now involves only two parameters, ψ_0 and ϵ . These can be related to the order parameter at the coexistence curve ϕ_∞ , the susceptibility χ , and the thermal correlation length ξ , as follows.¹⁰ From mean-field theory (recall that we quench from far above T_c to far below T_c) we have

$$\phi_\infty = (r/u)^{1/2}, \quad (3.9)$$

$$\chi = \frac{1}{a_0^d} \frac{k_B T}{(\partial^2 f / \partial \phi^2)_{\phi_\infty}} = \frac{1}{a_0^d} \frac{k_B T}{2r}, \quad (3.10)$$

and

$$\xi^{-2} = \frac{1}{K} \left[\frac{\partial^2 f}{\partial \phi^2} \right]_{\phi_\infty} = \frac{2r}{K}, \quad (3.11)$$

where a_0 is the underlying lattice spacing. Thus

$$\psi_0 = \phi_0 / \phi_\infty \quad (3.12)$$

and

$$\epsilon = \frac{1}{2^{d/2-1}} \frac{\chi}{\phi_\infty^2} \left[\frac{a_0}{\xi} \right]^d. \quad (3.13)$$

Note that ϵ is the parameter normally used in the Ginzburg criterion to determine the validity of a mean-field theory in critical phenomena. Near the critical point, if we assume hyperscaling, we obtain $\epsilon \propto (a_0/\xi_0)^d$ where ξ_0 is the amplitude of the correlation length. Thus $\epsilon \propto R^{-d}$, where R is the range of the force. Alternatively, this result follows directly from Eq. (2.5) since K is proportional to R^2 . It is worth noting that, in the notation of Langer *et al.*,¹⁰ $\epsilon \sim f_0^{-1}$, where f_0 is related to the range of the force. For the particular case of the Flory-Huggins free energy for polymers, Eq. (2.5), it can be shown that

$$\epsilon = \frac{2^d}{3} \left[\frac{k_B T}{K} \right]^{d/2} \frac{1}{N^{d/2-1} (v/v_{cr} - 1)^{(4-d)/2}}, \quad (3.14)$$

for $N_A = N_B = N$, where v_{cr} is the critical interaction parameter.³³ Thus for $d > 2$ and N large we find that $\epsilon \ll 1$ for polymers. It should also be noted that, from the definition of ϵ , Eq. (3.5), the perturbation theory can also be interpreted as a low-temperature or weak nonlinear coupling expansion.

As we will see, a crucial ingredient in the expansion in ϵ concerns initial conditions. By construction, $\psi(\tau=0) = 0$. The fluctuations around this value are given by the following. Let the initial temperature be $T' > T_c$. Then the coarse-grained free energy can safely be linearized to obtain

$$F[\phi, T'] = \int d^d r \left[\frac{K'}{2} (\nabla \phi)^2 + \frac{r'}{2} \phi^2 \right], \quad (3.15)$$

where r' is positive. The Langevin equation valid before the quench is

$$\frac{\partial \psi}{\partial \tau'}(\mathbf{x}', \tau') = \frac{1}{2} \nabla'^2 (-\nabla'^2 \psi + \psi) + \sqrt{\epsilon'} \mu, \quad (3.16)$$

where \mathbf{x}' and τ' are defined as in Eqs. (3.1) and (3.2) with $r \rightarrow r'$, $K \rightarrow K'$, and ψ defined as in Eq. (3.3). The parameter ϵ' can be shown to be related to ϵ via

$$\epsilon' = 2^{d/2-1} \frac{\chi(T')}{\chi(T)} \left[\frac{\xi(T)}{\xi(T')} \right]^d \epsilon, \quad (3.17)$$

i.e., $\epsilon' = O(\epsilon)$. One then straightforwardly obtains the high-temperature equilibrium solution

$$\langle \psi(\mathbf{q}) \psi(\mathbf{q}') \rangle = (2\pi)^d \delta(\mathbf{q} + \mathbf{q}') \frac{\epsilon'/2}{\frac{rK'}{r'K} q^2 + 1} \left[\frac{rK'}{r'K} \right]^{d/2}, \quad (3.18)$$

which is the Ornstein-Zernike function. Thus, at $\tau=0$, we have

$$\langle |\psi|^2 \rangle(\mathbf{q}, \tau=0) = \epsilon \frac{A}{q^2 + B}, \quad (3.19)$$

where $B = 2\xi^2(T)/\xi^2(T')$, and $A/B = \frac{1}{4}\chi(T')/\chi(T)$.

B. Perturbation expansion

The structure of the perturbation can now be obtained by assuming that

$$\psi = \psi^{(0)} + \epsilon^{1/2} \psi^{(1)} + \dots \quad (3.20)$$

A similar expansion for $\langle |\psi|^2 \rangle$ is then implicit. The equation of motion satisfied by $\psi^{(0)}$ is from Eq. (3.4),

$$\frac{\partial \psi^{(0)}}{\partial \tau} = \frac{1}{2} \nabla^2 [-\nabla^2 \psi^{(0)} - q_c^2 \psi^{(0)} + 3\psi_0 (\psi^{(0)})^2 + (\psi^{(0)})^3], \quad (3.21)$$

the solution of which is of the form $\psi^{(0)}(\mathbf{q}, \tau) = \psi(\mathbf{q}, \tau=0) f(\mathbf{q}, \tau)$. Therefore, since $\psi(\tau=0) \sim [\langle |\psi|^2 \rangle(\tau=0)]^{1/2}$, which is of order $\sqrt{\epsilon}$ from Eq. (3.19), we obtain

$$\psi^{(0)}(\mathbf{q}, \tau) = 0. \quad (3.22)$$

Furthermore, the expansion for the structure factor is

$$\langle |\psi|^2 \rangle = \epsilon \langle |\psi|^2 \rangle^{(1)} + \epsilon^{3/2} \langle |\psi|^2 \rangle^{(2)} + \dots \quad (3.23)$$

Let us now obtain the leading contribution to the structure factor in the expansion. From Eq. (3.4) we obtain

$$\frac{\partial}{\partial \tau} \langle |\psi|^2 \rangle^{(1)}(\mathbf{q}, \tau) = q^2 (q_c^2 - q^2) \langle |\psi|^2 \rangle^{(1)}(\mathbf{q}, \tau) + q^2 \quad (3.24)$$

in Fourier space, or

$$\langle |\psi|^2 \rangle^{(1)}(\mathbf{q}, \tau) = \frac{A}{q^2 + B} e^{q^2 (q_c^2 - q^2) \tau} - \left[\frac{1 - e^{q^2 (q_c^2 - q^2) \tau}}{q^2 - q_c^2} \right]. \quad (3.25)$$

Thus to leading order in the expansion in the range of the force we reobtain the result of Cahn-Hilliard-Cook theory, Eq. (2.10).

Before proceeding with the formal expansion, given in

the next section, it is useful to reconsider the nonlinear contributions entering the equation for the structure factor, such as $\langle \psi^3 \psi \rangle$. The exact equation for this can be shown to be

$$\begin{aligned} \frac{\partial}{\partial \tau} \langle \psi^2(\mathbf{x}_1, \tau) \psi(\mathbf{x}_2, \tau) \rangle &= -\frac{3}{2} \langle \psi^2(\mathbf{x}_1) [\nabla_1^2 (q_c^2 + \nabla_1^2) \psi(\mathbf{x}_1)] \psi(\mathbf{x}_2) \rangle - \frac{1}{2} \nabla_2^2 (q_c^2 + \nabla_2^2) \langle \psi^3(\mathbf{x}_1) \psi(\mathbf{x}_2) \rangle \\ &+ \frac{9\psi_0}{2} \langle \psi^2(\mathbf{x}_1) [\nabla_1^2 \psi^2(\mathbf{x}_1)] \psi(\mathbf{x}_2) \rangle + \frac{3\psi_0}{2} \nabla_2^2 \langle \psi^3(\mathbf{x}_1) \psi^2(\mathbf{x}_2) \rangle \\ &+ \frac{3}{2} \langle \psi^2(\mathbf{x}_1) [\nabla_1^2 \psi^3(\mathbf{x}_1)] \psi(\mathbf{x}_2) \rangle + \frac{1}{2} \nabla_2^2 \langle \psi^3(\mathbf{x}_1) \psi^3(\mathbf{x}_2) \rangle \\ &- 3\epsilon \langle \psi^2(\mathbf{x}_1) \rangle \nabla_1^2 \delta(\mathbf{x}_1 - \mathbf{x}_2) - 3\epsilon \langle \psi(\mathbf{x}_1) \psi(\mathbf{x}_2) \rangle \lim_{\mathbf{x}_1 \rightarrow 0} \nabla_1^2 \delta(\mathbf{x}_1) . \end{aligned} \quad (3.26)$$

The important thing to note here is that, despite the expansion in ϵ , one cannot disentangle the gradients from the correlation functions in terms like $\langle \psi^2(\nabla^2 \psi^3) \psi \rangle$. This is essentially because these terms involve coupling to a higher-order distribution function in the hierarchy (the gradient explores the region $\mathbf{x} + d\mathbf{x}$, as well as the point \mathbf{x} itself). As noted at the beginning of this section, we believe that this subtle coupling is not adequately handled in earlier theories. This coupling is accounted for in our calculation below. Indeed, although our treatment (to order ϵ^2) is essentially equivalent to a factorization decoupling of higher-order moments, a careful analysis of the many-body correlation functions is necessary to consistently effect this decoupling. (The systematic calculation is given in the next section.) It should be noted that the result does not reduce to that obtained by Langer,^{9,37} precisely because of that coupling which is absent from Langer's treatment.

Finally, let us consider the time domain of validity of our expansion. Firstly, we recover the estimate of the region of validity of the linear theory,^{12,13,38} Eq. (3.25). Roughly speaking, this result will be incorrect when the next term in the series is important. If we ignore the Cook term for simplicity, the maximum time τ_{\max} for the validity of the linear Cahn-Hilliard-Cook theory is given by

$$\epsilon e^{q^2(q_c^2 - q^2)\tau_{\max}} \sim O(\epsilon^{3/2}), \quad (3.27)$$

where $O(\epsilon^{3/2})$ is the next term in the expansion. Thus we have, recalling that $\epsilon \propto R^{-d}$,

$$\tau_{\max} \sim \ln R . \quad (3.28)$$

A more convincing demonstration of this result is given in Binder's papers.^{13,39}

The validity of an expansion in thermal noise intensity has been discussed in analogous dynamical problems, where spatial inhomogeneities are irrelevant (laser problems, or well-stirred chemical reactions).⁴⁰ There it is known that the expansion becomes a singular perturbation

theory for late times, where each term in the series has the same importance. Thus, to be conservative, we would expect the expansion in ϵ to be accurate over the early-time regime given by Eq. (3.28).⁴¹ We speculate that if $\tau_{\max} = C \ln R$, then by calculating an increasing number of terms in the series we increase the value of the prefactor C , without changing the essential dependence of τ_{\max} upon R .

IV. FIRST-ORDER CALCULATION

We will now obtain a relation for the n -body correlation function within the perturbation expansion. Although we only wish to obtain the structure factor, it is necessary to consider the more general case. It will prove convenient to introduce a diagrammatic representation, similar to that used by Kawasaki.³⁶

The scaled Fokker-Planck equation for the probability density, corresponding to Eq. (3.4), is

$$\frac{\partial \rho}{\partial \tau} = \int d^d r D \rho , \quad (4.1)$$

where the operator D is given by

$$D \equiv -\nabla^2 \left[\frac{1}{2} \frac{\delta}{\delta \psi} (-q_c^2 - \nabla^2 + 3\psi_0 \psi^2 + \psi^3) + \frac{\epsilon}{2} \frac{\delta^2}{\delta \psi^2} \right] . \quad (4.2)$$

Thus the n -body equal-time correlation function is given by

$$\frac{\partial}{\partial \tau} \langle \psi(\mathbf{x}_1, \tau) \cdots \psi(\mathbf{x}_n, \tau) \rangle = \langle \tilde{D} \psi(\mathbf{x}_1, \tau) \cdots \psi(\mathbf{x}_n, \tau) \rangle , \quad (4.3)$$

where \tilde{D} denotes the adjoint of D . After some algebra we obtain

$$\begin{aligned} \frac{\partial}{\partial \tau} \langle \psi(\mathbf{x}_1, \tau) \cdots \psi(\mathbf{x}_n, \tau) \rangle &= \frac{1}{2}(\gamma_{\nabla_1} + \gamma_{\nabla_2} + \cdots) \langle \psi(\mathbf{x}_1, \tau) \cdots \psi(\mathbf{x}_n, \tau) \rangle + \frac{3\psi_0}{2} \nabla_1^2 \langle \psi^2(\mathbf{x}_1, \tau) \cdots \psi(\mathbf{x}_n, \tau) \rangle \\ &+ \cdots + \frac{1}{2} \nabla_1^2 \langle \psi^3(\mathbf{x}_1, \tau) \cdots \psi(\mathbf{x}_n, \tau) \rangle + \cdots + \epsilon \nabla_1^2 \delta(\mathbf{x}_1 - \mathbf{x}_2) \langle \psi(\mathbf{x}_3, \tau) \cdots \psi(\mathbf{x}_n, \tau) \rangle + \cdots, \end{aligned} \quad (4.4)$$

where

$$\gamma_{\nabla} \equiv -\nabla^2(q_c^2 + \nabla^2), \quad (4.5)$$

and the sums in the first three terms consist of n terms, while the sum in the last term consists of $\frac{1}{2}n(n-1)$ terms (with no double counting).

A useful change of variables, after Fourier transformation, is given by

$$\langle \psi(\mathbf{q}_1, \tau) \cdots \psi(\mathbf{q}_n, \tau) \rangle \equiv \epsilon^{n/2} e^{(\gamma_{q_1} + \gamma_{q_2} + \cdots)\tau/2} S_n(\mathbf{q}_1, \dots, \mathbf{q}_n, \tau). \quad (4.6)$$

Again, after some algebra, we obtain

$$\begin{aligned} S_n(\mathbf{q}_1, \dots, \mathbf{q}_n, \tau) &= S_n(\mathbf{q}_1, \dots, \mathbf{q}_n, 0) + \int_0^\tau d\tau' [V_2(\mathbf{q}_1, \mathbf{q}_2, \tau') S_{n-2}(\mathbf{q}_3, \dots, \mathbf{q}_n, \tau') + \cdots] \\ &+ \epsilon^{1/2} \int_0^\tau d\tau' \int \int \frac{d^d k_1}{(2\pi)^d} \frac{d^d k_2}{(2\pi)^d} [V_3(\mathbf{q}_1, \mathbf{k}_1, \mathbf{k}_2, \tau') S_{n+1}(\mathbf{k}_1, \mathbf{k}_2, \mathbf{q}_2, \dots, \mathbf{q}_n, \tau') + \cdots] \\ &+ \epsilon \int_0^\tau d\tau' \int \int \int \frac{d^d k_1}{(2\pi)^d} \frac{d^d k_2}{(2\pi)^d} \frac{d^d k_3}{(2\pi)^d} [V_4(\mathbf{q}_1, \mathbf{k}_1, \mathbf{k}_2, \mathbf{k}_3, \tau') S_{n+2}(\mathbf{k}_1, \mathbf{k}_2, \mathbf{k}_3, \mathbf{q}_2, \dots, \mathbf{q}_n, \tau') + \cdots], \end{aligned} \quad (4.7)$$

which gives a formal solution for $S_n(t)$. The second term on the right-hand side involves a sum over $\frac{1}{2}n(n-1)$ pairs, while the last two terms involve a sum over n terms. The "vertices" are given by the following:

$$V_2(\mathbf{q}_1, \mathbf{q}_2, \tau) = 2q_1^2 e^{-\gamma_{q_1}\tau} (2\pi)^d \delta(\mathbf{q}_1 + \mathbf{q}_2), \quad (4.8)$$

which is due to thermal noise,

$$\begin{aligned} V_3(\mathbf{q}_1, \mathbf{k}_1, \mathbf{k}_2, \tau) &= 3\psi_0 q_1^2 e^{-(\gamma_{q_1} - \gamma_{k_1} - \gamma_{k_2})\tau/2} \\ &\times (2\pi)^d \delta(\mathbf{q}_1 - \mathbf{k}_1 - \mathbf{k}_2), \end{aligned} \quad (4.9)$$

which is the "three-rayed" interaction, and

$$\begin{aligned} V_4(\mathbf{q}_1, \mathbf{k}_1, \mathbf{k}_2, \mathbf{k}_3, \tau) &= -q_1^2 e^{-(\gamma_{q_1} - \gamma_{k_1} - \gamma_{k_2} - \gamma_{k_3})\tau/2} \\ &\times (2\pi)^d \delta(\mathbf{q}_1 - \mathbf{k}_1 - \mathbf{k}_2 - \mathbf{k}_3), \end{aligned} \quad (4.10)$$

which is the four-rayed interaction. The expansion in ϵ for $S_n(t)$ can be written as

$$S_n(\tau) = S_n^{(0)}(\tau) + \epsilon^{1/2} S_n^{(1)}(\tau) + \cdots, \quad (4.11)$$

where we have suppressed wave-number dependences for simplicity. From Eqs. (3.3) and (3.19), the initial conditions are such that

$$S_1(q, \tau=0) = 0 \quad (4.12)$$

and

$$S_2(q_1, q_2, \tau=0) = (2\pi)^d \delta(\mathbf{q}_1 + \mathbf{q}_2) \frac{A}{q_1^2 + B},$$

while the higher-order moments are determined by a

Gaussian distribution, $\exp(-F/k_B T)$, given by Eq. (3.16). Thus we finally obtain the equations

$$S_n^{(0)}(\tau) = S_n(0) + \int_0^\tau d\tau' [V_2(\tau') S_{n-2}^{(0)}(\tau') + \cdots], \quad (4.13)$$

$$\begin{aligned} S_n^{(1)}(\tau) &= \int_0^\tau d\tau' [V_2(\tau') S_{n-2}^{(1)}(\tau') + \cdots] \\ &+ \int_0^\tau d\tau' [V_3(\tau') S_{n+1}^{(0)}(\tau') + \cdots], \end{aligned} \quad (4.14)$$

and, for $m > 1$,

$$\begin{aligned} S_n^{(m)}(\tau) &= \int_0^\tau d\tau' [V_2(\tau') S_{n-2}^{(m)}(\tau') + \cdots] \\ &+ \int_0^\tau d\tau' [V_3(\tau') S_{n+1}^{(m-1)}(\tau') + \cdots] \\ &+ \int_0^\tau d\tau' [V_4(\tau') S_{n+2}^{(m-2)}(\tau') + \cdots]. \end{aligned} \quad (4.15)$$

These equations naturally lend themselves to a diagrammatic representation for $S_2(t)$, from which the structure factor is obtained in Eq. (4.6). In Fig. 1 we display the diagrams corresponding to $S_2^{(0)}(q_1, q_2, t)$. These should be compared to Eq. (4.13). The diagram shown in Fig. 1(a) is due to initial conditions, while the diagram in Fig. 1(b) has a two-rayed vertex at a time τ_1 . From the definition of V_2 , we obtain

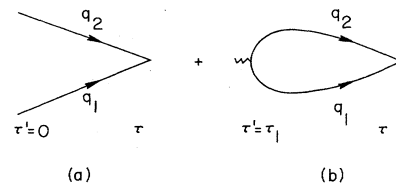


FIG. 1. Diagrams giving $S_2^{(0)}(\mathbf{q}_1, \mathbf{q}_2, \tau)$.

$$S_2^{(0)}(\mathbf{q}_1, \mathbf{q}_2, \tau) = \left[\frac{A}{q_1^2 + B} + \frac{1 - e^{-\gamma_{q_1} \tau}}{\gamma_{q_1}} \right] (2\pi)^d \delta(\mathbf{q}_1 + \mathbf{q}_2). \quad (4.16)$$

[Note that $S_0(t) = 1$, by normalization.] Thus Fig. 1 corresponds to the Cahn-Hilliard-Cook theory, in a rather abstract form.

In Fig. 2, the diagrams giving $S_2^{(2)}(\mathbf{q}_1, \mathbf{q}_2, \tau)$ for a symmetric quench ($\psi_0 = 0$) are displayed. (The additional diagrams needed for an off-symmetric quench are given in the Appendix.) Consider the second diagram. It has two vertices, one of which is the V_2 thermal noise vertex at time τ_1 , while the other is the V_4 interaction vertex at time τ_2 . All the "extra" lines, labeled k_1 , k_2 , and k_3 , correspond to integrated wave numbers. For example, this diagram gives a contribution

$$\int_0^\tau d\tau_2 \left[\int \int \int \frac{d^d k_1}{(2\pi)^d} \frac{d^d k_2}{(2\pi)^d} \frac{d^d k_3}{(2\pi)^d} V_4(\mathbf{q}_1, \mathbf{k}_1, \mathbf{k}_2, \mathbf{k}_3, \tau_2) \right] \int_0^{\tau_2} d\tau_1 V_2(\mathbf{q}_2, \mathbf{k}_3, \tau_1) S_2(\mathbf{k}_1, \mathbf{k}_2, 0). \quad (4.17)$$

The $S_2(\mathbf{k}_1, \mathbf{k}_2, \tau = 0)$ factor comes from the two dangling lines at $\tau = 0$. The symmetry factor of 6 gives the number of "topologically equivalent" ways one could create this diagram. The remainder of the analysis involves only considerable algebra. The eventual result we obtain is

$$S_2^{(2)}(\mathbf{q}_1, \mathbf{q}_2, \tau) = \frac{3q_1^2}{2\pi^2} \left[\frac{A^2}{q_1^2 + B} I_1 + \frac{A}{q_1^2 + B} I_2 + Aq_1^2 I_3 + q_1^2 I_4 + q_1^2 I_5 \right] (2\pi)^d \delta(\mathbf{q}_1 + \mathbf{q}_2), \quad (4.18)$$

where for $d = 3$ the integrals are given by (Λ is the ultraviolet cutoff)

$$I_1 = \int_0^\Lambda \frac{k^2 dk}{k^2 + B} \frac{1 - e^{\gamma_k \tau}}{\gamma_k},$$

$$I_2 = \int_0^\Lambda \frac{k^4 dk}{\gamma_k^2} (1 + \gamma_k \tau - e^{\gamma_k \tau}),$$

$$I_3 = \frac{1}{\gamma_{q_1}} \left[I_1 - \int_0^\Lambda \frac{k^2 dk}{k^2 + B} \frac{1 - e^{(\gamma_k - \gamma_{q_1}) \tau}}{\gamma_k - \gamma_{q_1}} \right],$$

$$I_4 = \frac{1}{\gamma_{q_1}} \left[I_2 - \int_0^\Lambda \frac{k^4 dk}{\gamma_k + \gamma_{q_1}} \left[\frac{1 - e^{\gamma_k \tau}}{\gamma_k} + \frac{1 - e^{\gamma_{q_1} \tau}}{\gamma_{q_1}} \right] \right],$$

and

$$I_5 = \frac{1}{\gamma_{q_1}} \int_0^\Lambda \frac{k^4 dk}{\gamma_k} \left[\frac{e^{-\gamma_{q_1} \tau}}{\gamma_k + \gamma_{q_1}} (1 - e^{(\gamma_k + \gamma_{q_1}) \tau}) - \frac{1}{\gamma_k - \gamma_{q_1}} (1 - e^{(\gamma_k - \gamma_{q_1}) \tau}) \right].$$

These integrals were evaluated numerically to obtain the results given in the following section. Thus from Eqs. (4.6), (4.16), and (4.18) (we note that $S_2^{(1)} = 0$) we obtain

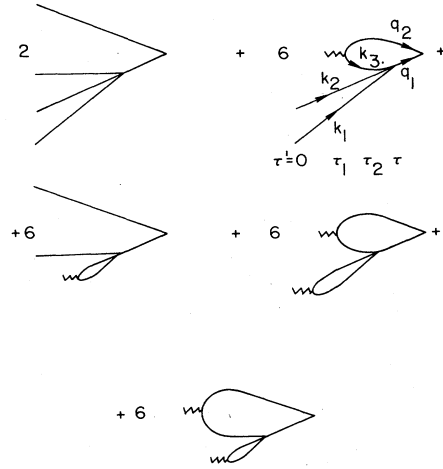


FIG. 2. Diagrams giving $S_2^{(2)}(\mathbf{q}_1, \mathbf{q}_2, \tau)$ for a symmetric quench, $\psi_0 = 0$.

our main result, namely the structure factor $\langle |\psi|^2 \rangle$ to order ϵ^2 .

Before presenting those results, given in the following section, we have some final comments on the expansion in ϵ . Since we have only obtained results to order ϵ^2 , our treatment corresponds to a time-dependent Gaussian form for the probability distribution function. Thus we obtain coarsening in the initial stages, but the distribution function does not become bimodal. Since the series is apparently alternating, we would have to go to order ϵ^4 to obtain a bimodal distribution. We note, however, that an analysis to order ϵ^n requires approximately 10^{n-1} diagrams. We also note that it may be possible to undertake a singular perturbation theory for late times and sum an infinite class of these diagrams. Thus was done for the nonconserved case (in a certain weak-coupling, long-time limit) by Kawasaki, Yalabik, and Gunton.⁴²

V. RESULTS AND DISCUSSION

We have numerically evaluated the result for the structure factor, derived in the previous section, for different times following a symmetric quench ($\psi_0 = 0$). The ultraviolet wave-number cutoff was chosen to be 10^0 $\Lambda = [(\partial^2 f / \partial \psi^2) | \psi = 1]^{1/2}$, while the initial conditions, Eq. (3.19), were chosen to be $A = B = 1$. Before discussing our results, it is worth relating ϵ to the range of the force more explicitly. In three dimensions, as discussed above,

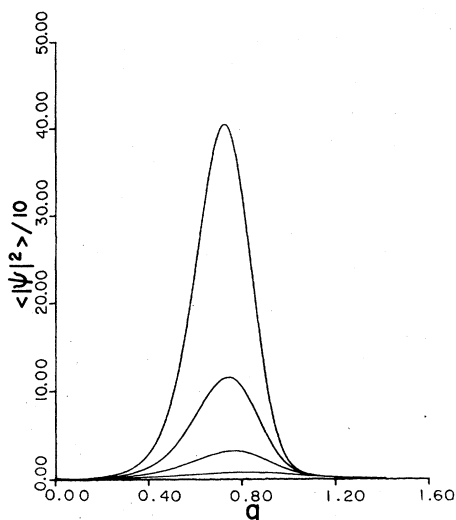


FIG. 3. Structure factor $\langle |\psi|^2 \rangle(q, \tau)$ vs q . Cahn-Hilliard-Cook theory ($\epsilon=0$). Times shown are $\tau=5, 10, 15$, and 20 .

the range of the force is $R \propto \epsilon^{-1/3}$. For the nearest-neighbor Ising model, where we assume that $R \equiv 1$, ϵ is estimated¹⁰ to be 3.63. Thus we are led to the relation

$$R \approx 1.54/\epsilon^{1/3}. \quad (5.1)$$

From this we obtain, for the values of ϵ studied below ($\epsilon=0.02, 0.04$, and 0.1), the ranges of interaction which are $R=3.3, 4.5$, and 5.6 , respectively. A typical polymer-polymer blend, with a chain length of roughly 400 "lattice spacings," would have $R \sim 20$. It should also be noted that the real time t , in terms of the scaled time τ , is

$$t \sim R^2 \tau. \quad (5.2)$$

Thus even though the scaled times studied below are $\tau \leq 20$, the real time in an experimental system could be of significant duration.

In Fig. 3 we show the Cahn-Hilliard-Cook structure factor (that is, the $\epsilon=0$ result) for times $\tau=5, 10, 15$, and 20 . In Fig. 4 we present our result with $\epsilon=0.02$ for the same times. Not surprisingly, the growth rate is slower in Fig. 4 where the range of the force is finite, although large. As mentioned above, the correction term we have calculated to the theory of Cahn *et al.* is negative for all wave numbers and all times. The slower growth can also be seen in the direct comparison given in Fig. 5 for $\epsilon=0.02, 0.04$, and 0.1 , at $\tau=10$. It should also be noted that, in Fig. 4, even though the peak of the structure factor is growing, the large q tail is decreasing. Hence, the curve actually crosses itself. This interesting feature has been observed in both Monte Carlo and experimental studies.²²⁻²⁵ It originates from nonlinear effects, and thus is absent in the Cahn-Hilliard-Cook theory.

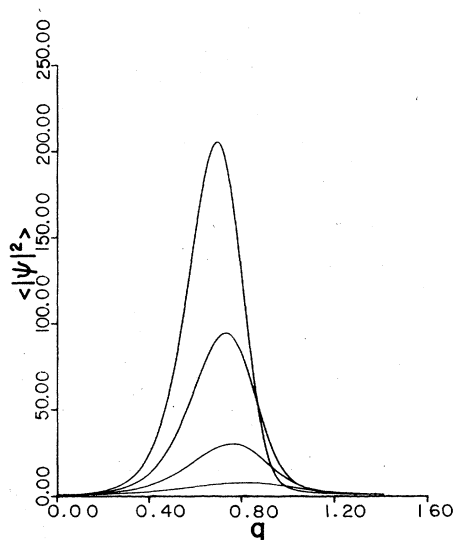


FIG. 4. Structure factor $\langle |\psi|^2 \rangle(q, \tau)$ vs q . Our result with $\epsilon=0.02$. Times shown are $\tau=5, 10, 15$, and 20 . Growth is slower than in Fig. 3.

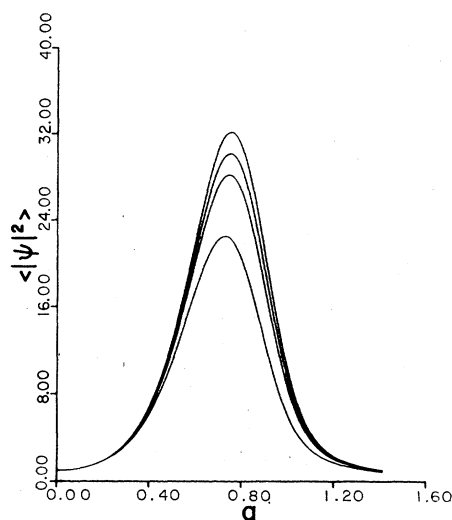


FIG. 5. Structure factor $\langle |\psi|^2 \rangle(q, \tau)$ vs q . All curves at time $\tau=10$. From top, curves are $\epsilon=0, 0.02, 0.04$, and 0.1 .

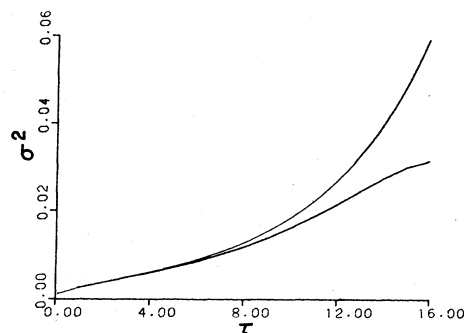


FIG. 6. Effective Gaussian width $\sigma^2(\tau)$ for $\epsilon=0$ (top) and $\epsilon=0.04$.

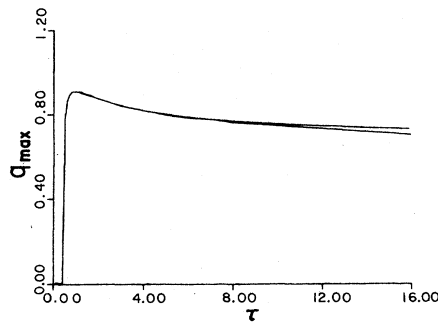


FIG. 7. Wave number of maximum intensity, q_{\max} vs τ for $\epsilon=0$ (top) and $\epsilon=0.04$.

In Fig. 6 we plot the effective Gaussian width, $\sigma^2(t)$, of the one-body distribution function for both $\epsilon=0$ and 0.04. The width is given by the sum rule

$$\sigma^2(\tau) = \int \frac{d^3q}{(2\pi)^3} \langle |\psi|^2 \rangle(q, \tau).$$

This shows the coarsening given by the correction term to the theory of Cahn *et al.* Note that in the linear theory $\sigma^2(t)$ increases exponentially, so that the one-body distribution function never equilibrates. The coarsening can also be seen in Fig. 7 where we plot the position of the maximum intensity versus time.

As discussed above, we expect the valid time regime for this perturbation theory to be $\tau \leq \ln(1/\epsilon)$. This is in agreement with what we find by determining the time at which the Cahn-Hilliard-Cook theory differs significantly (more than approximately 10%) from the result of perturbation theory. Binder's¹³ estimate of a maximum time τ_{\max} for the validity of linear theory is $\tau_{\max} \approx -4 \ln 3 \epsilon$ in

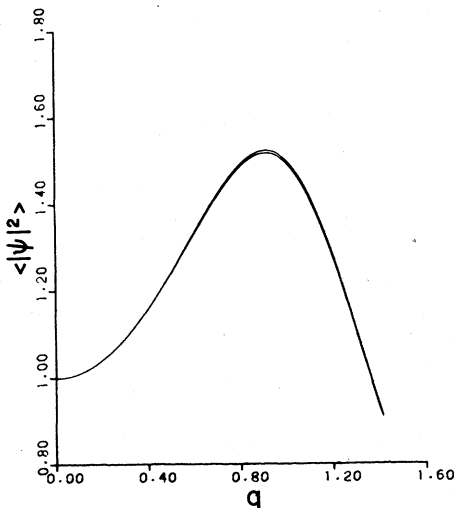


FIG. 8. Structure factor $\langle |\psi|^2 \rangle(q, \tau)$ vs q for $\tau=1$. Top curve is Cahn-Hilliard-Cook result ($\epsilon=0$). Indistinguishable bottom two curves are our result and that of Langer-Baron-Miller for $\epsilon=0.04$.

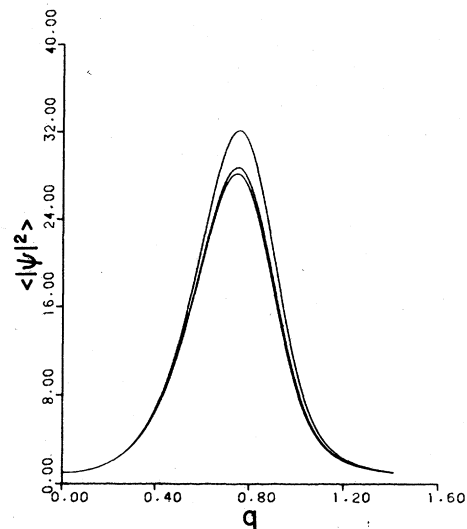


FIG. 9. Structure factor $\langle |\psi|^2 \rangle(q, \tau)$ vs q for $\tau=10$. Top curve is Cahn-Hilliard-Cook result. Next curve is Langer-Baron-Miller result ($\epsilon=0.04$). Bottom curve is our result ($\epsilon=0.04$).

our units, for a symmetric quench. For $\epsilon=0.02, 0.04$, and 0.1, these times are $\tau_{\max} \approx 11, 8$, and 5, respectively, which are in agreement with our results.

In Figs. 8 and 9 we compare Cahn-Hilliard-Cook theory, our theory, and the Langer-Baron-Miller theory¹⁰ for the structure factor, at two different times, $\tau=1$ and 10. (We have used the same initial conditions for all three theories, and the same range of the force, $\epsilon=0.04$, for our theory and the theory of Langer *et al.*) For $\tau=1$, in Fig. 8, our theory and the theory of Langer *et al.* practically coincide. The reason for this is as fol-

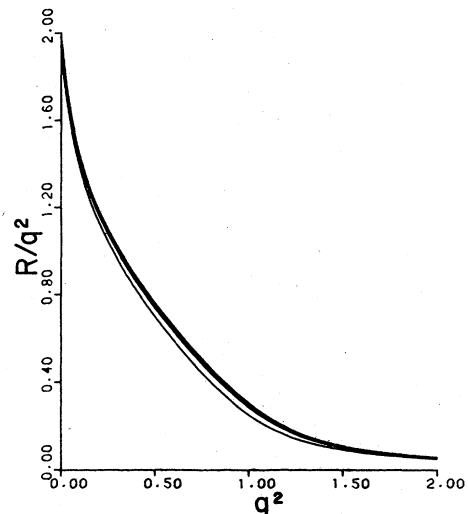


FIG. 10. R/q^2 vs q^2 for $\tau=10$ where the amplification factor is $R \equiv (1/\tau) \ln \langle |\psi|^2 \rangle(q, \tau)$. Curves from top to bottom are $\epsilon=0, 0.02, 0.04$, and 0.1.

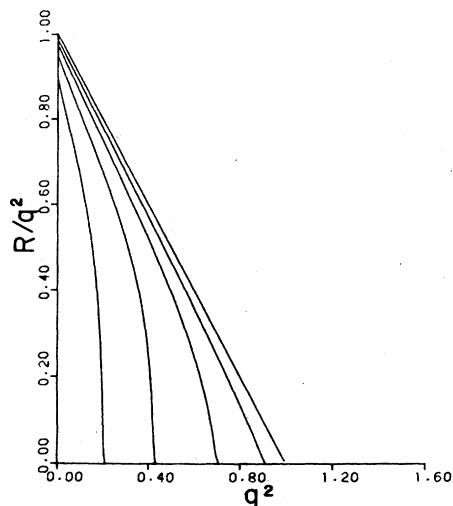


FIG. 11. R/q^2 vs q^2 , where the Cook term has been set to zero. The amplification factor is $R \equiv (1/\tau) \ln \langle |\psi|^2 \rangle(q, \tau)$. Top curve is Cahn-Hilliard result ($\epsilon=0$). Bottom curves are our result from $\epsilon=0.04$, for times $\tau=5, 10, 15$, and 20 .

lows. If one expands our equations of motion in time, one obtains a decoupling of wave-number modes for very early times similar to that assumed by Langer *et al.* For later times, however, the coupling of modes becomes important and so our theory yields results which are different from those of Langer *et al.*, as can be seen in Fig. 9. The coupling of modes in our result is seen more easily in the plots given in Figs. 10 and 11 discussed below. A careful experiment, on a system with long-range forces, could, we suppose, distinguish between our theory and those of Cahn *et al.* and Langer *et al.*

In Figs. 10 and 11 we plot the logarithm of the structure factor, divided by $q^2\tau$, versus q^2 . This is a standard plot used in the metallurgical literature to test the Cahn-Hilliard-Cook theory. In Fig. 10 the plot is for $\tau=10$, with $\epsilon=0, 0.02, 0.04$, and 0.1 . In Fig. 11 we have subtracted the Cook term from the scattering intensity so that the plot will give a straight line with no time dependence, for the Cahn-Hilliard theory, $\epsilon=0$. The plot is for $\epsilon=0$ and $\epsilon=0.04$, for the times $\tau=5, 10, 15$, and 20 . In the context of the linear theory, the critical wave number q_c is determined by the intercepts of that straight line, and so (for off-symmetric quenches) one obtains the classical spinodal curve. We find two noteworthy differences from linear theory for nonzero ϵ in Fig. 11. Firstly, as time increases, there is a departure from the straight line as q increases. This is a consequence of the coupling of wave-number modes in our theory, as discussed above. The bending in Fig. 11 would be absent from a similar

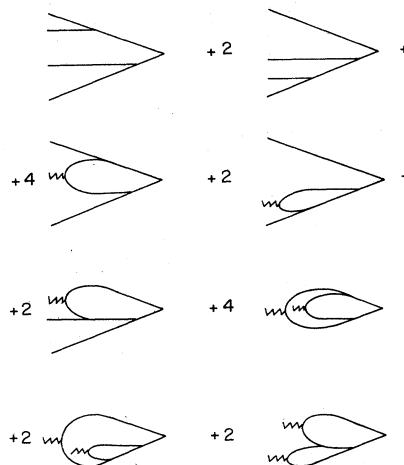


FIG. 12. Additional diagrams, for an off-symmetric quench, for $S_2^{(2)}(q_1, q_2, \tau)$ in Fig. 2 or Eq. (4.18).

plot of the result of the Langer-Bar-on-Miller theory. Secondly, we find that the $q=0$ intercept is clearly time dependent. (This also follows in the analyses of Langer and co-workers.⁸⁻¹⁰) Thus if one insists on defining an effective critical wave number by this criterion, it must be time dependent.

The implication of this result is clear. If one extends our numerical calculation to off-symmetric quenches (which we have not done) one would obtain a time-dependent spinodal. We do not believe that this has physical significance: The result is a consequence of forcing a pseudo-equilibrium quantity, the classical spinodal line, onto a dynamical problem. Thus, in our opinion, one cannot consistently define a sharp spinodal line.³ Only systems with an infinite range of interaction will have this sharp transition between unstable and metastable states. Some ways to characterize the gradual transition, which is observed experimentally, have been given by other authors.²⁴⁻³¹

To conclude, we have presented a perturbative analysis for the early stages of phase separation in spinodal decomposition. Our treatment should be valid for systems with long-range interactions. An experimental or computer simulation study of such a system would be of considerable interest.

ACKNOWLEDGMENTS

This work was supported by National Science Foundation Grant No. DMR-8312958. M.G. is supported by the Natural Sciences and Engineering Research Council (NSERC) of Canada. J. V. is supported by Comissió Interdepartamental de Recerca i Innovació Tecnològica (CIRIT) (Generalitat de Catalunya).

APPENDIX

In this appendix we report the results of the additional contributions to $S_2^{(2)}(q_1, q_2, \tau)$ in Eq. (4.18) for an off-symmetric quench. The eight nonvanishing diagrams are shown in Fig. 12. In the same manner as the evaluation summarized in Sec. IV, we obtain (where $\mathbf{q}_- \equiv \mathbf{q}_1 - \mathbf{k}$)

$$S' = (2\pi)^d \delta(\mathbf{q}_1 + \mathbf{q}_2) 9\psi_0^2 q_1^2 I',$$

with

$$\begin{aligned}
I' = & q_1^2 A^2 \int \frac{d^d k}{(2\pi)^d} \frac{1}{(k^2 + B)(q_-^2 + B)} \left[\frac{1 - e^{(-\gamma_{q_1} + \gamma_k + \gamma_{q_-})\tau/2}}{-\gamma_{q_1} + \gamma_k + \gamma_{q_-}} \right]^2 \\
& + \frac{4A^2}{q_1^2 + B} \int \frac{d^d k}{(2\pi)^d} \frac{q_-^2}{(k^2 + B)} \left[\frac{1 - e^{(-\gamma_{q_1} + \gamma_k + \gamma_{q_-})\tau/2}}{\gamma_k^2 - (\gamma_{q_1} - \gamma_{q_-})^2} - \frac{1 - e^{\gamma_k \tau}}{2\gamma_k(-\gamma_{q_-} + \gamma_k + \gamma_{q_1})} \right] \\
& + 4q_1^2 A \int \frac{d^d k}{(2\pi)^d} \frac{q_-^2}{k^2 + B} \frac{1}{\gamma_{q_-}} \left[\frac{1}{2} \left[\frac{1 - e^{(-\gamma_{q_1} + \gamma_k + \gamma_{q_-})\tau/2}}{-\gamma_{q_1} + \gamma_k + \gamma_{q_-}} \right]^2 - \frac{1 - e^{(-\gamma_{q_1} + \gamma_k + \gamma_{q_-})\tau/2}}{(-\gamma_{q_1} + \gamma_k)^2 - \gamma_{q_-}^2} \right. \\
& \quad \left. + \frac{1 - e^{(-\gamma_{q_1} + \gamma_k)\tau}}{2(-\gamma_{q_1} + \gamma_k)(-\gamma_{q_1} + \gamma_k - \gamma_{q_-})} \right] \\
& + \frac{2A}{q_1^2 + B} \int \frac{d^d k}{(2\pi)^d} \frac{k^2 q_-^2}{\gamma_k} \left[\frac{1 - e^{(-\gamma_{q_1} + \gamma_k + \gamma_{q_-})\tau/2}}{\gamma_k^2 - (\gamma_{q_-} - \gamma_{q_1})^2} - \frac{1 - e^{\gamma_k \tau}}{2\gamma_k(-\gamma_{q_-} + \gamma_k + \gamma_{q_1})} \right. \\
& \quad \left. + \frac{1 + (-\gamma_{q_1} + \gamma_k + \gamma_{q_-})\tau/2 - e^{(-\gamma_{q_1} + \gamma_k + \gamma_{q_-})\tau/2}}{(-\gamma_{q_1} + \gamma_k + \gamma_{q_-})^2} \right] \\
& + \frac{2q_1^2 A}{\gamma_{q_1}} \int \frac{d^d k}{(2\pi)^d} \frac{q_-^2}{k^2 + B} \left[-\frac{2\gamma_{q_1}(1 - e^{(-\gamma_{q_1} + \gamma_k + \gamma_{q_-})\tau/2})}{[(-\gamma_{q_-} + \gamma_k)^2 - \gamma_{q_1}^2](-\gamma_{q_1} + \gamma_k + \gamma_{q_-})} \right. \\
& \quad \left. - \frac{1 - e^{\gamma_k \tau}}{2\gamma_k(-\gamma_{q_-} + \gamma_k + \gamma_{q_1})} + \frac{1 - e^{(-\gamma_{q_1} + \gamma_k)\tau}}{2(-\gamma_{q_1} + \gamma_k)(-\gamma_{q_-} + \gamma_k - \gamma_{q_1})} \right] \\
& + 4q^2 \int \frac{d^d k}{(2\pi)^d} \frac{k^2 q_-^2}{\gamma_k} \left[\frac{\gamma_k}{2\gamma_{q_-}(\gamma_k + \gamma_{q_-})} \left[\frac{1 - e^{(-\gamma_{q_1} + \gamma_k + \gamma_{q_-})\tau/2}}{-\gamma_{q_1} + \gamma_k + \gamma_{q_-}} \right]^2 \right. \\
& \quad - \left[\frac{1}{\gamma_{q_-} [(-\gamma_{q_1} + \gamma_k)^2 - \gamma_{q_-}^2]} + \frac{1}{(\gamma_k + \gamma_{q_-}) [-\gamma_{q_1}^2 + (\gamma_k + \gamma_{q_-})^2]} \right] \\
& \quad \times [1 - e^{(-\gamma_{q_1} + \gamma_k + \gamma_{q_-})\tau/2}] + \frac{1 - e^{(-\gamma_{q_1} + \gamma_k)\tau}}{2\gamma_{q_-}(-\gamma_{q_1} + \gamma_k)(-\gamma_{q_1} + \gamma_k - \gamma_{q_-})} \\
& \quad \left. - \frac{1 - e^{-\gamma_{q_1} \tau}}{2\gamma_{q_1}(\gamma_k + \gamma_{q_-})(\gamma_{q_1} + \gamma_k + \gamma_{q_-})} \right] \\
& + \frac{2q_1^2}{\gamma_{q_1}} \int \frac{d^d k}{(2\pi)^d} \frac{k^2 q_-^2}{k^2 + B} \left[\frac{1 + (-\gamma_{q_1} + \gamma_k + \gamma_{q_-})\tau/2 - e^{(-\gamma_{q_1} + \gamma_k + \gamma_{q_-})\tau/2}}{\gamma_k(-\gamma_{q_1} + \gamma_k + \gamma_{q_-})^2} - \frac{1 - e^{-\gamma_{q_1} \tau}}{2\gamma_{q_1}(\gamma_{q_1} + \gamma_k)(\gamma_{q_1} + \gamma_k + \gamma_{q_-})} \right. \\
& \quad \left. - \frac{\gamma_{q_1}(1 - e^{\gamma_k \tau})}{2\gamma_k^2(\gamma_{q_1} + \gamma_k)(-\gamma_{q_-} + \gamma_k + \gamma_{q_1})} \right]
\end{aligned}$$

$$\begin{aligned}
& + \left[\frac{\gamma_{q_1}}{\gamma_k(\gamma_{q_1} + \gamma_k)[\gamma_k^2 - (-\gamma_{q_1} + \gamma_{q_-})^2]} - \frac{1}{(\gamma_{q_1} + \gamma_k)[\gamma_k + \gamma_{q_-}]^2 - \gamma_{q_1}^2} \right] (1 - e^{(-\gamma_{q_1} + \gamma_k + \gamma_{q_-})\tau/2}) \\
& + 2q_1^2 \int \frac{d^d k}{(2\pi)^d} \frac{k^2 q_-^2}{\gamma_k} \left[\frac{1 - e^{(-\gamma_{q_1} + \gamma_k)\tau}}{2\gamma_{q_1}(-\gamma_{q_1} + \gamma_k)(-\gamma_{q_-} - \gamma_{q_1} + \gamma_k)} - \frac{1 - e^{\gamma_k \tau}}{2\gamma_{q_1}(\gamma_{q_1} + \gamma_k)(-\gamma_{q_-} + \gamma_{q_1} + \gamma_k)} \right. \\
& \quad - \frac{1 - e^{-\gamma_{q_1} \tau}}{2\gamma_{q_1}(\gamma_{q_1} + \gamma_k)(\gamma_{q_-} + \gamma_{q_1} + \gamma_k)} + \left. \frac{\gamma_k}{\gamma_{q_1}(\gamma_{q_1} + \gamma_k)[\gamma_k^2 - (-\gamma_{q_1} + \gamma_{q_-})^2]} \right. \\
& \quad - \frac{1}{\gamma_{q_1}[(\gamma_k - \gamma_{q_1})^2 - \gamma_{q_-}^2]} \\
& \quad \left. - \frac{1}{(\gamma_{q_1} + \gamma_k)[(\gamma_k + \gamma_{q_-})^2 - \gamma_{q_1}^2]} \right] \\
& \quad \times (1 - e^{(-\gamma_{q_1} + \gamma_k + \gamma_{q_-})\tau/2})
\end{aligned}$$

*Permanent address: Departamento de Física Teórica, Universidad de Barcelona, Diagonal 647, Barcelona 28, Spain.

¹J. D. Gunton, M. San Miguel, and P. S. Sahni, in *Phase Transitions and Critical Phenomena*, edited by C. Domb and J. L. Lebowitz (Academic, London, 1983), Vol. 8.

²K. Binder, in *Lecture Notes for NATO Advanced Research Workshop, Condensed Matter Research Using Neutrons, Today and Tomorrow* (Plenum, New York, in press).

³J. D. Gunton, in *Early Stages of Decomposition in Alloys*, edited by M. H. Ashby (Pergamon, London, in press).

⁴V. P. Skripov and A. V. Skirpov, *Usp. Fiz. Nauk* **128**, 193 (1979) [*Sov. Phys.—Usp.* **22**, 389 (1979)].

⁵J. W. Cahn, *Trans. Metall. Soc. AIME* **242**, 166 (1968), and references therein.

⁶J. E. Hilliard, in *Phase Transformations*, edited by H. I. Aronson (American Society for Metals, Metals Park, Ohio, 1970), and references therein.

⁷H. E. Cook, *Acta Metall.* **18**, 297 (1970).

⁸J. S. Langer, in *Fluctuations, Instabilities and Phase Transitions*, edited by T. Riste (Plenum, New York, 1975), p. 19, and references therein.

⁹J. S. Langer, *Ann. Phys. (N.Y.)* **65**, 53 (1971).

¹⁰J. S. Langer, M. Bar-on, and H. D. Miller, *Phys. Rev. A* **11**, 1417 (1975).

¹¹I. M. Lifshitz and V. V. Slyozov, *J. Phys. Chem. Solids* **19**, 35 (1961); K. Kawasaki and T. Ohta, *Prog. Theor. Phys.* **68**, 129 (1982); *Physica* **118A**, 175 (1983).

¹²A. Z. Patashinskii and V. L. Pokrovskii, *Fluktuatsionnaya Teoriya Fazovykh Prekhodov* (Fluctuation Theory of Phase Transitions) (Nauka, Moscow, 1975). See also Ref. 4.

¹³K. Binder, *J. Chem. Phys.* **79**, 6387 (1983); *Phys. Rev. A* **29**, 341 (1984).

¹⁴J. C. LaSalle, S. Spooner, and L. H. Schwartz (unpublished).

¹⁵S. Katano and M. Iizumi (unpublished).

¹⁶H. L. Snyder, P. Meakin, and S. Reich, *Macromolecules* **16**, 757 (1983); *J. Chem. Phys.* **78**, 3334 (1983); H. L. Snyder and P. Meakin, *ibid.* **79**, 5588 (1983); *J. Polym. Sci. C* (to be published).

¹⁷T. P. Russell, G. Hadziioannou, and W. Warburton, *Macromolecules* (to be published); G. Ronca and T. P. Russell, *ibid.*

¹⁸S. Nojima, K. Tsutsumi, and T. Nose, *Polymer J.* **14**, 225 (1982).

¹⁹T. Hashimoto, J. Kumaki, and H. Kawai, *Macromolecules* **16**, 641 (1983).

²⁰Although interactions are short ranged in polymers, an effective long-range force appears in the coarse-grained free energy which is approximately the square root of the length of a polymer chain. See Eq. (3.14).

²¹D. W. Heermann, *Phys. Rev. Lett.* **52**, 1126 (1984).

²²M. Hennion, D. Ronzaud, and P. Guyot, *Acta Metall.* **30**, 599 (1982).

²³P. Guyot and J. P. Simon, in *Solid-State Phase Transformations*, edited by I. Aaronset *et al.* (American Institute of Mechanical Engineers, New York, 1982), p. 325.

²⁴J. L. Lebowitz, J. Marro, and M. H. Kalos, *Acta Metall.* **30**, 297 (1982).

²⁵P. Fratzl, J. L. Lebowitz, J. Marro, and M. H. Kalos, *Acta Metall.* **30**, 297 (1982).

²⁶K. Binder and D. Stauffer, *Adv. Phys.* **25**, 343 (1976).

²⁷K. Binder, *Phys. Rev. B* **15**, 4425 (1976).

²⁸P. Mirolid and K. Binder, *Acta Metall.* **25**, 1435 (1977).

²⁹D. W. Heermann and W. Klein, *Phys. Rev. B* **27**, 1732 (1983).

³⁰W. Klein and C. Unger, *Phys. Rev. B* **28**, 445 (1983).

³¹D. W. Heermann, *Z. Phys. B* (to be published).

³²P. C. Hohenberg and B. I. Halperin, *Rev. Mod. Phys.* **49**, 435 (1977).

³³For the free energy, Eq. (2.5), the critical values of c and v are

$$c_{\text{cr}} = (N_B)^{1/2} [(N_A)^{1/2} + (N_B)^{1/2}]^{-1}$$

and

$$v_{\text{cr}} = [(N_A)^{1/2} + (N_B)^{1/2}]^2 (2N_A N_B)^{-1}.$$

The corresponding values of r and u in Eq. (2.3) are

$$r = 2k_B T v_{\text{cr}} (v/v_{\text{cr}} - 1)$$

and

$$u = \frac{4}{3} k_B T v_{\text{cr}}^2 (N_A N_B)^{1/2}.$$

Note that the dynamical model [Eq. (2.1)] would neglect any hydrodynamic effects in polymer blends. The model also neglects any concentration dependence in the coefficient of the gradient term K , and any spatial dependence of the mobility M . The consequences of removing these last two assumptions have been analyzed by Binder, within the linear theory (Ref. 13).

³⁴The Cahn-Hilliard theory predicts no coarsening: The maximum of the structure factor occurs at a time-dependent wave

number q_{max} . The inclusion of the Cook term, which is due to thermal fluctuations, leads to a time-dependent q_{max} . A discussion of the Cook term is given in Ref. 4.

³⁵C. Billotet and K. Binder, *Z. Phys. B* **32**, 195 (1979).

³⁶K. Kawasaki, *Prog. Theor. Phys.* **57**, 410 (1977); **58**, 175 (1977).

³⁷This is in contrast to $d=0$ systems, where there are no gradient terms. There a factorization decoupling, as done by Langer, would be equivalent to a systematic approximation to order ϵ^2 .

³⁸See also R. Petschek and H. Metiu, *J. Chem. Phys.* **79**, 1948 (1983).

³⁹Equation (3.28) admits an appealing physical interpretation of τ_{max} as the time needed for the system to leave the immediate vicinity of the unstable state. In fact, a mean-first-passage-time calculation [F. Haake, J. W. Haus, and R. Glauber, *Phys. Rev. A* **23**, 3855 (1981)] shows that this time has the asymptotic behavior $\tau_{\text{max}} \sim \ln \epsilon^{-1}$, for all ϵ .

⁴⁰M. Suzuki, in *Order and Fluctuations in Equilibrium and Nonequilibrium Statistical Mechanics*, edited by G. Nicolis, G. Dewel, and J. W. Turner (Wiley, New York, 1978), p. 299.

⁴¹This seems to be born out by the mean-first-passage-time calculation mentioned in Ref. 39: The asymptotic behavior of τ_{max} is not modified by the consideration of nonlinear terms. The escape from the unstable state occurs for $\tau < \tau_{\text{max}}$, and is dominated by linear terms. In this regime nonlinear effects can be considered perturbatively.

⁴²K. Kawasaki, M. C. Yalabik, and J. D. Gunton, *Phys. Rev. A* **17**, 455 (1978).